Electronic Supplementary Information (ESI)

for

Muffin-like lanthanide complexes with an N_5O_2-donor macrocyclic ligand showing field-induced single-molecule magnet behaviour

Peter Antal, Bohuslav Drahoš, Radovan Herchel and Zdeněk Trávníček*

Department of Inorganic Chemistry, Regional Centre of Advanced Technologies and Materials, Palacký University, 17. listopadu 12, CZ-771 46 Olomouc, Czech Republic

*zdenek.travnicek@upol.cz

Table of contents

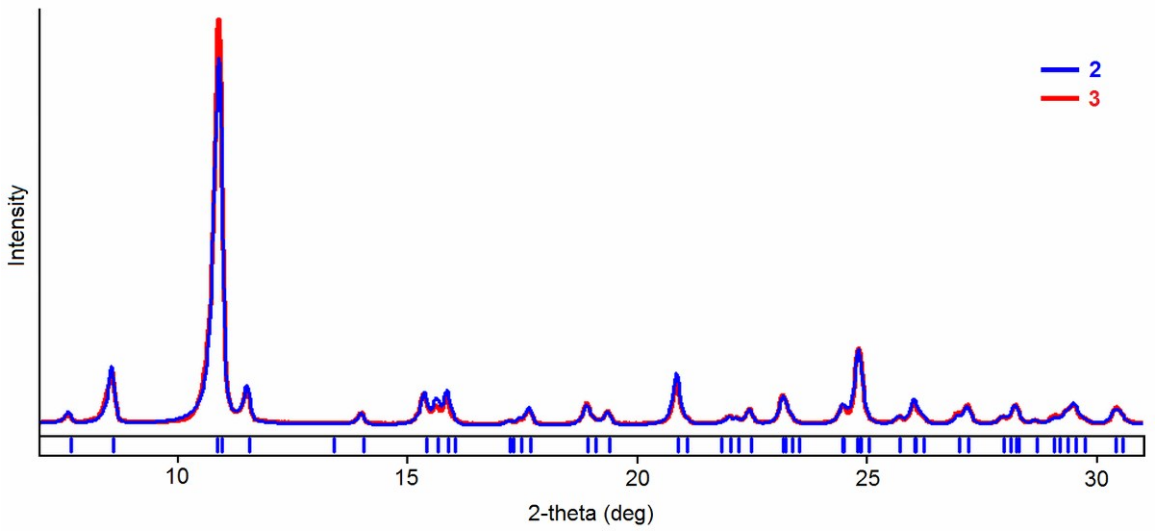

Figure S1. A comparison of the X-ray powder diffraction patterns of compounds **2** (blue) and **3** (red).

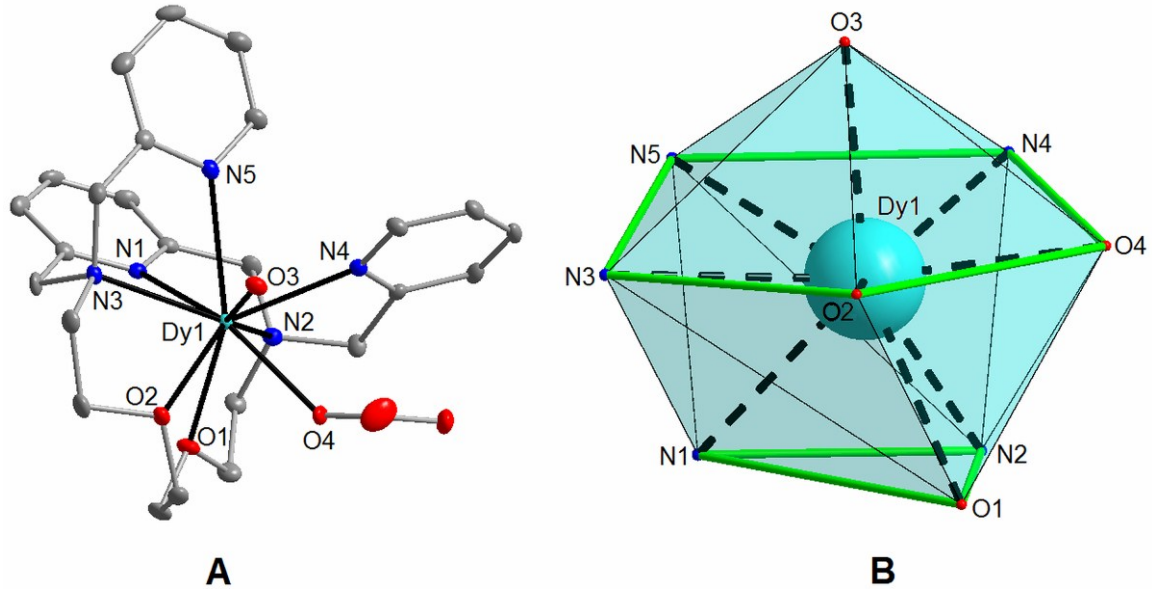

Figure S2. (**A**) Molecular structure of the $[Dy(\mathbf{L})(H_2O)(NO_3)]^{2+}$ complex cation in **2**. Thermal ellipsoids are drawn with 50% probability level. The hydrogen atoms are omitted for clarity. (**B**) The coordination geometry of the $[DyN_5O_4]$ core in **2**.

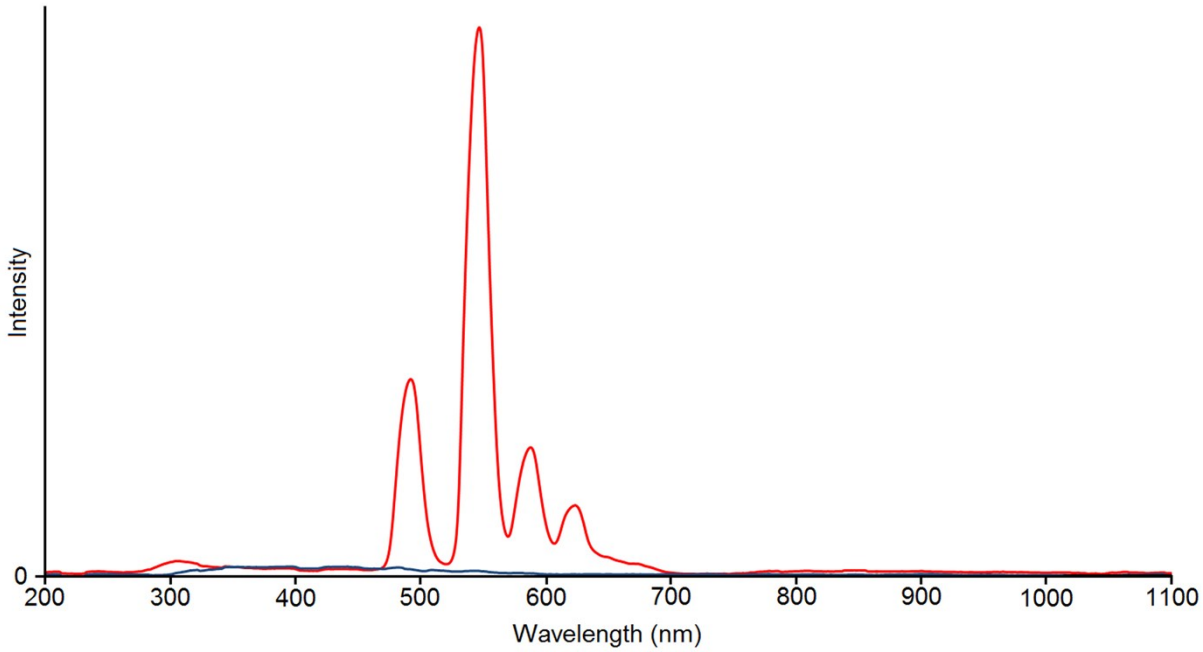

Figure S3. Photoluminescence spectra of **1** (red line) and Tb^{III} complex of the parent 15-N_3O_2 macrocyclic ligand without 2-pyridylmethyl pendant arms (dark blue) measured in acetonitrile/methanol solution (c = 1 × 10^{-3} mol dm^{-3}) at room temperature. The Tb^{III} complex of 15-N_3O_2 was prepared *in situ* by mixing of equimolar amounts of $Tb(NO_3)_3 \cdot 5H_2O$ and 15-N_3O_2.

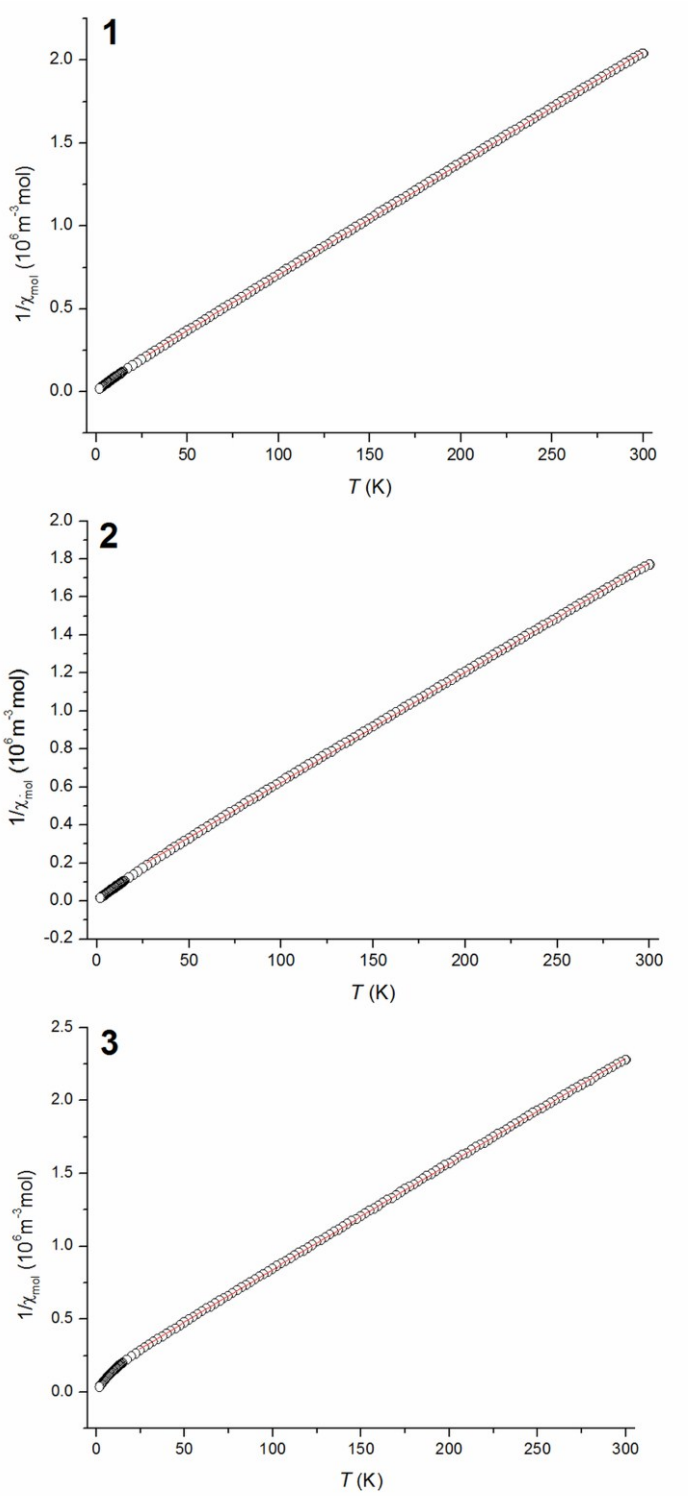

Figure S4. The analysis of the molar susceptibilities for **1**–**3** with Curie-Weiss law in the temperature range of 25–300 K. Empty circles – experimental data, full lines – calculated data.

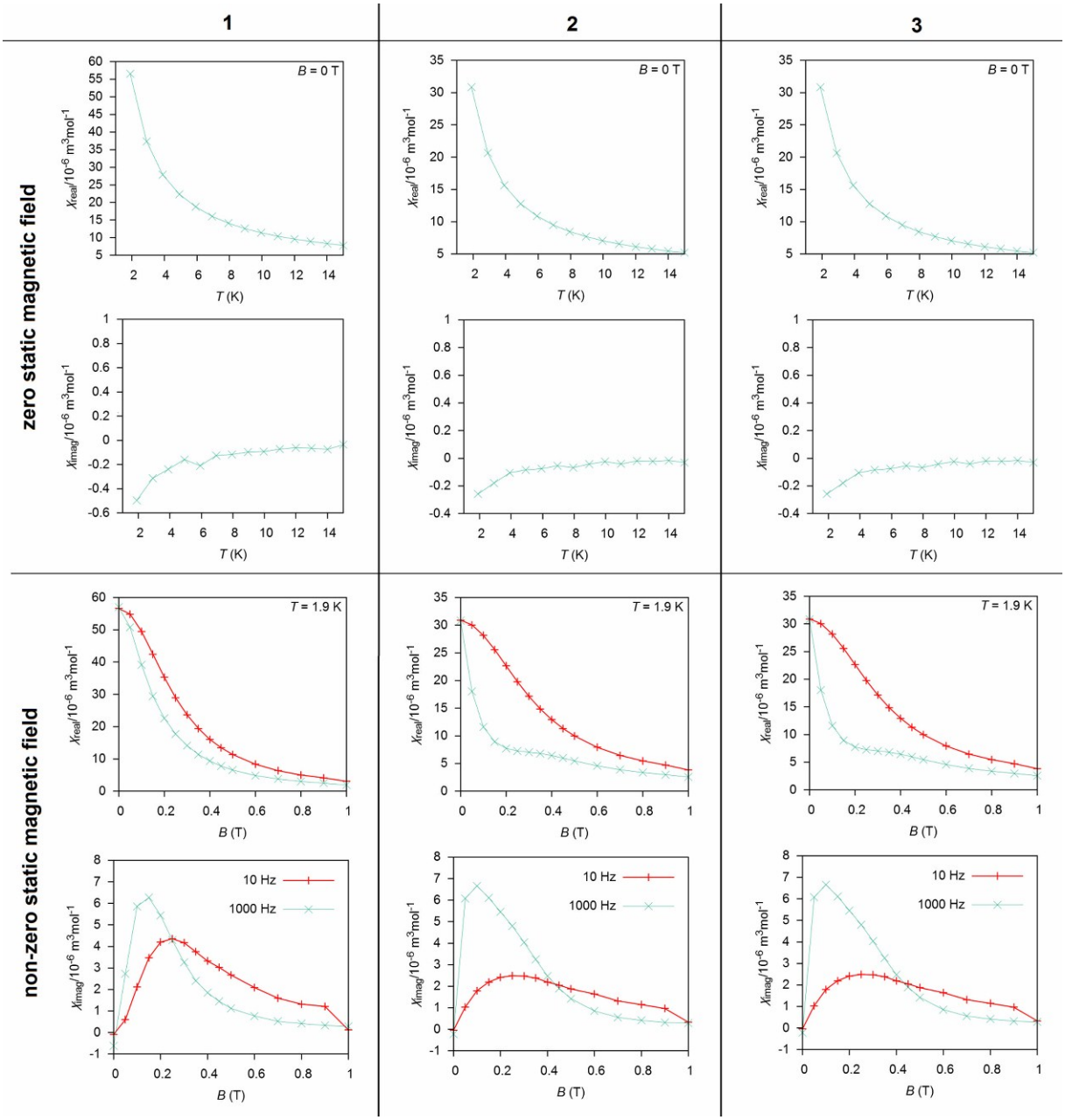

Figure S5. The in-phase χ_{real} and out-of-phase χ_{imag} molar susceptibilities for **1**–**3** at zero static magnetic field (left) and in non-zero static magnetic field B = 0.1 T (right).

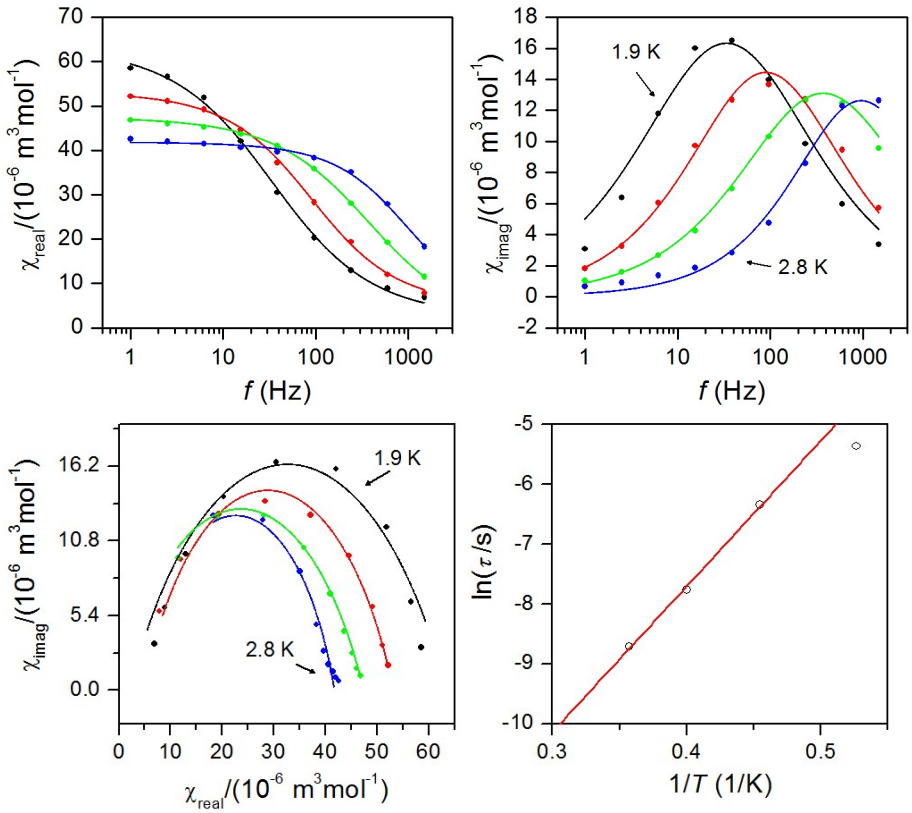

Figure S6. *Top*: frequency dependence of in-phase χ_{real} and out-of-phase χ_{imag} molar susceptibilities for **2** at B_{DC} = 0.1 T. Full points – experimental data, full lines – fitted data using eq. 6. *Bottom*: Argand (Cole-Cole) plot and fit of resulting relaxation times according to Arrhenius law (red line), where only data having maxima in the Argand diagram were used.

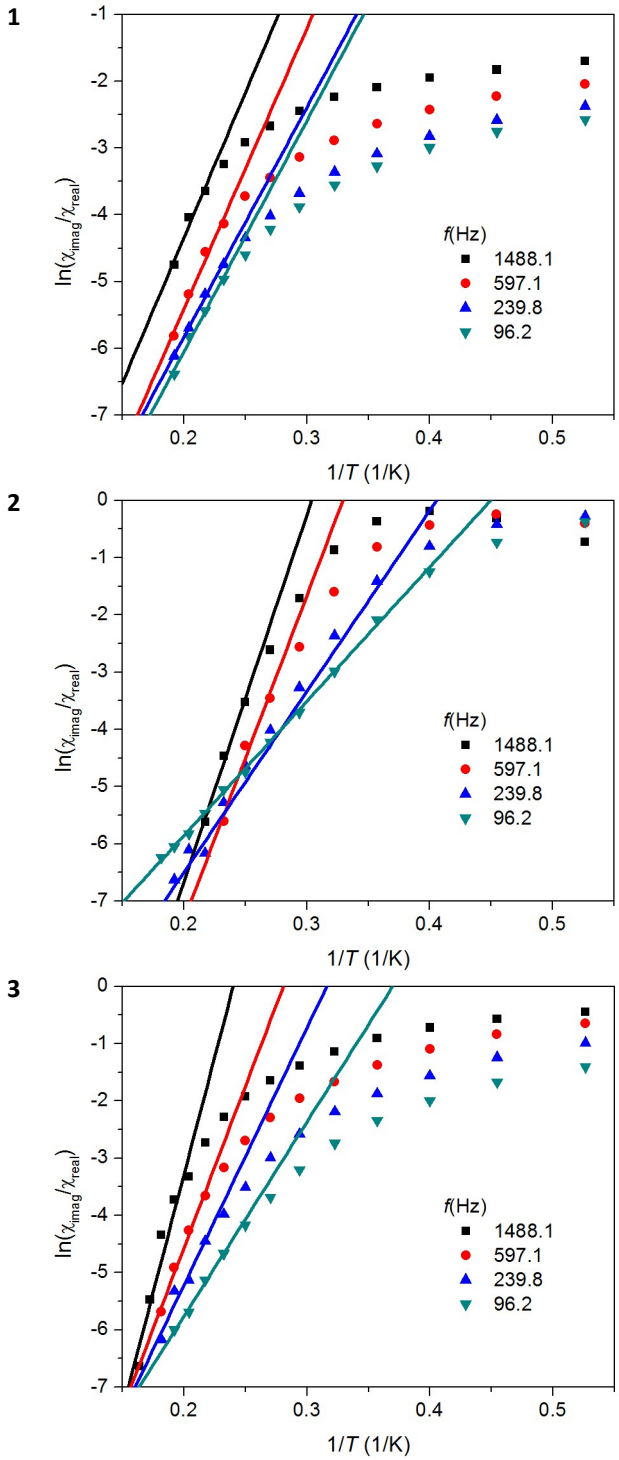

Figure S7. Analysis of in-phase χ_{real} and out-of-phase χ_{imag} molar susceptibilities for **1**–**3** measured at the applied external field B_{DC} = 0.1 T according to eq. 2. Full points – experimental data, full lines – calculated data.

2

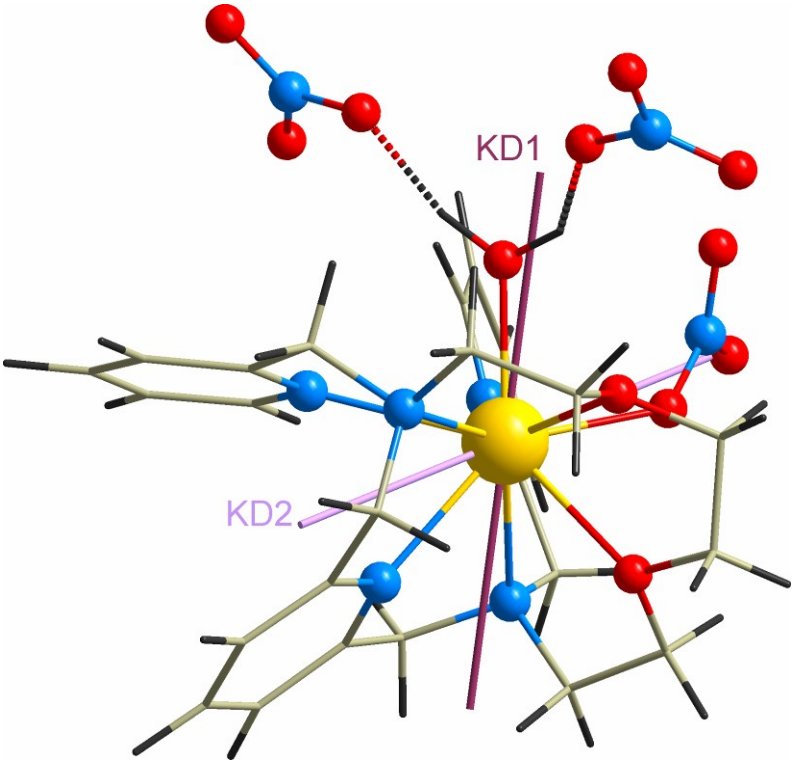

3

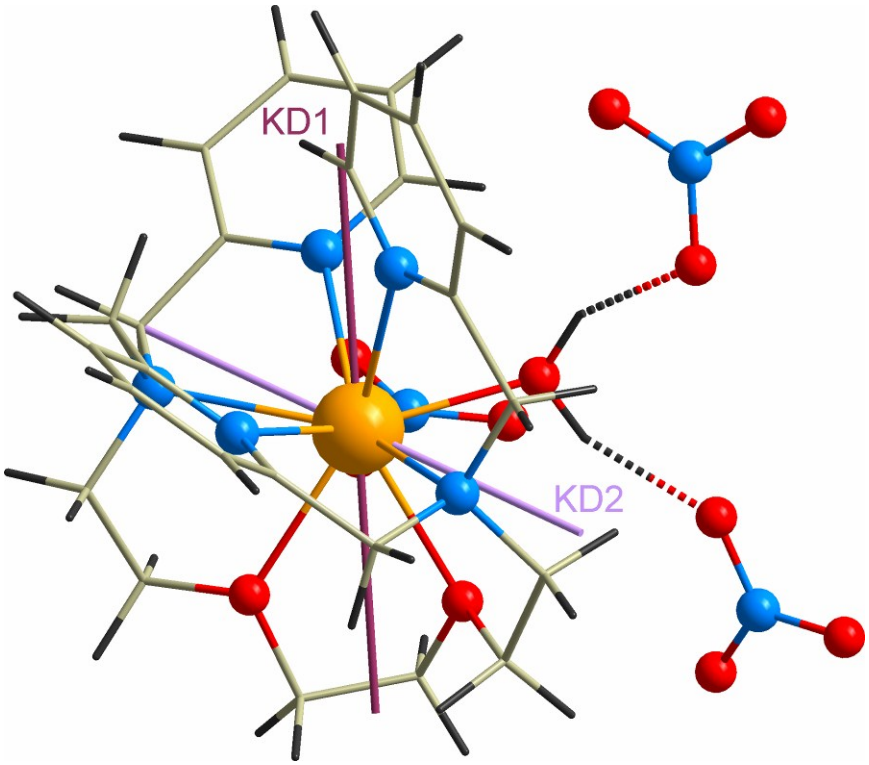

Figure S8. Representations of the geometries of [Dy(**L**)(H_2O)(NO_3)](NO_3)$_2$ (**2**, *top*) and [Er(**L**)(H_2O)(NO_3)](NO_3)$_2$ (**3**, *bottom*) which were used in CASSCF calculations and easy axes of the ground state (KD1) and first excited (KD2) Kramer doublets. Dotted lines represent the O–H···O hydrogen bonds.

Table S1. Results of continuous shape calculations using program Shape 2.1 for complexes **1** and **2**.[a]

	Tb(III)	Dy(III)
CN = 9[b]		
EP-9	34.013	34.075
OPY-9	20.955	20.930
HBPY-9	16.739	16.822
JTC-9	14.546	14.581
JCCU-9	9.017	9.046
CCU-9	7.831	7.883
JCSAPR-9	2.748	2.698
CSAPR-9	1.785	1.748
JTCTPR-9	4.116	4.043
TCTPR-9	1.764	1.722
JTDIC-9	11.193	11.214
HH-9	10.386	10.420
MFF-9	1.045	1.042

[a] the listed values correspond to the deviation between the ideal and real coordination polyhedra, the lowest values are given in red colour.

[b] EP-9 = enneagon, OPY-9 = octagonal pyramid, HBPY-9 = heptagonal bipyramid, JTC-9 = Johnson triangular cupola J3, JCCU-9 = capped cube J8, CCU-9 = spherical-relaxed capped cube, JCSAPR-9 = capped square antiprism, CSAPR-9 = spherical capped square antiprism, JTCTPR-9 = tricapped trigonal prism J51, TCTPR-9 = spherical tricapped trigonal prism, JTDIC-9 = tridiminished icosahedron, HH-9 = hula-hoop, MFF-9 = muffin.

Table S2. Selected hydrogen bonds and other non-covalent contacts in the crystal structures of **1** and **2**.

D–H···A[a]	*d*(D···H) [Å]	*d*(H···A) [Å]	*d*(D···A) [Å]	ϑ(D···H) [°]
1				
O(3)–H(3V)···O(12)	0.82	2.05	2.746	142.7
O(3)–H(3W)···O(8)	0.83	1.87	2.660	158.4
C(11)–H(11A)···O(11)[b]	0.95	2.51	3.150	124.7
C(13)–H(13A)···O(5)	0.95	2.54	3.315	139.0
C(17)–H(17A)···O(5)[c]	0.95	2.51	3.339	146.1
C(24)–H(24A)···O(12)[d]	0.95	2.50	3.382	154.4
C(19)–H(19A)···N(5)	0.95	2.54	3.156	122.5
C(3A)-H(3A)···N(8)[e]	0.99	2.45	3.325	147.6
2				
O(3)–H(3V)···O(11)	0.82	2.03	2.750	145.1
O(3)–H(3W)···O(8)	0.83	1.90	2.662	151.9
C(11)–H(11A)···O(5)	0.95	2.54	3.316	138.8
C(13)–H(13A)···O(10)[f]	0.95	2.50	3.143	125.1
C(17)–H(17A)···O(11)[g]	0.95	2.51	3.391	153.9
C(18)–H(18A)···O(8)[h]	0.95	2.67	3.356	130.0
C(25)–H(25A)···N(4)	0.95	2.54	3.148	122.3
C(8A)–H(8A)···N(8)[e]	0.99	2.45	3.326	147.4

[a]Symmetry transformations used to generate equivalent atoms: [b] x, $-y+1$, $z+1/4$. [c] x, $-y$, $z+1/4$. [d] $-x$, $y-1$, $z-1/4$. [e] $x+1$, $-y+1$, $z+1/4$. [f] x, $-y+2$, $z+1/4$. [g] $-x+1$, $y+1$, $z-1/4$. [h] $x-1$, $-y+1$, $z+1/4$.

Table S3. Parameters of one-component Debye model for the Dy^{III} complex **2** derived according to eq.1 in the main text.

T/K	χ_S/(10^{-6} m^3mol^{-1})	χ_T/(10^{-6} m^3mol^{-1})	α	τ/(10^{-4} s)
1.9	2.148	63.462	0.378	46.817
2.2	4.743	53.209	0.316	17.579
2.5	0.002	47.464	0.358	4.242
2.8	3.734	41.807	0.255	1.648
3.1	21.593	39.314	0.258	1.984

Table S4 Energy levels (cm^{-1} or K) of the lowest ligand field multiplets in zero magnetic field derived from CASSCF/DKH2/SINGLE_ANISO calculations of [Tb(**L**)(H_2O)(NO_3)](NO_3)$_2$ **1** with the respective *g*-factors derived for each Kramer's doublet with the effective spin 1/2.

Energy (cm^{-1})	Energy (K)	g_X	g_Y	g_Z
0.000	0.000	0.000000103	0.000000273	16.675081359
0.695	1.000			
23.137	33.289			
27.367	39.375			
67.869	97.648			
83.357	119.931			
99.152	142.657			
126.438	181.915			
140.271	201.818			
199.698	287.319			
204.141	293.712			
376.397	541.548			
376.714	542.004			

Table S5 Energy levels (cm^{-1} or K) of the lowest ligand field multiplets in zero magnetic field derived from CASSCF/DKH2/SINGLE_ANISO calculations of [Dy(**L**)(H_2O)(NO_3)](NO_3)$_2$ **2** with the respective *g*-factors derived for each Kramer's doublet with the effective spin 1/2.

Energy (cm^{-1})	Energy (K)	g_X	g_Y	g_Z
0	0.000	0.123208278	0. 401662841	19.214014361
38.243	55.023	0.356141137	0.826105795	18.433216066
113.567	163.397	3.918803592	4.811990429	12.560372284
150.540	216.592	1.850824694	2.945792689	13.510993216
190.234	273.703	7.954737034	5.663277147	3.008111909
296.665	426.832	0.459719199	0.947727009	14.713092241
332.608	478.546	0.139527338	0.371625830	18.288261450
391.878	563.822	0.247472833	0.431595384	17.241550158

Table S6 Energy levels (cm^{-1} or K) of the lowest ligand field multiplets in zero magnetic field derived from CASSCF/DKH2/SINGLE_ANISO calculations of [Er(**L**)(H_2O)(NO_3)](NO_3)$_2$ **3** with respective *g*-factors derived for each Kramer's doublet with the effective spin 1/2.

Energy (cm^{-1})	Energy (K)	g_X	g_Y	g_Z
0.000	0.000	1.123801903	2.180915307	13.849557162
47.928	68.957	0.771485743	2.219025733	11.176748604
69.830	100.469	3.012527039	5.223582763	8.198121785
133.220	191.673	1.949056313	2.887259140	10.494647672
159.320	229.225	1.280224132	4.288008015	8.089948499
213.909	307.766	8.967453663	5.443248836	0.007673973
269.653	387.968	0.225782405	3.578347299	7.125835001
319.015	458.989	1.252656637	5.766399195	12.068693060